DRAG REDUCTION IN AIRCRAFT MODEL USING ELLIPTICAL WINGLET

Prithvi Raj Arora[1], A. Hossain[1], Prasetyo Edi[1], A.A. Jaafar[1], Thamir S. Younis[2] and M. Saleem[1]

[1]*Department of Aerospace Engineering, Universiti Putra Malaysia, 43400 UPM, Serdang, Selangor*

[2]*Department of Mechanical Engineering, Universiti Putra Malaysia, 43400 UPM, Serdang, Selangor*

ABSTRACT

Aerodynamic characteristics for the aircraft model with NACA (National Advisory Committee for Aeronautics) wing No. 65-3-218 have been studied using subsonic wind tunnel of 1000 mm x 1000 mm rectangular test section and 2500 mm long of Aerodynamics Laboratory Faculty of Engineering (Universiti Putra Malaysia). Six components wind tunnel balance is used for measuring lift, drag and pitching moment. Tests are conducted on the aircraft model with and without winglet of two configurations at Reynolds numbers 1.7 x 10^5, 2.1 x 10^5, and 2.5 x 10^5. Lift curve slope increases more with the addition of the elliptical winglet and at the same time the drag decreases more for the aircraft model with elliptical shaped winglet giving an edge over the aircraft model without winglet as far as Lift/Drag ratio for the elliptical winglet is considered. Elliptical winglet of configuration 2 (Winglet inclination 60^0) has, overall, the best performance, giving about 6% increase in lift curve slope as compared to without winglet and it is giving the best lift/drag ratio.

Keywords : *Induced Drag, Lift Curve Slope, Wind Tunnel Balance, Winglet*

INTRODUCTION

The aerodynamic efficiency and drag of aircraft wing shapes depend on profile drag as well as on the induced drag. By introducing various types of wingtip devices in wingtip region the aerodynamic efficiency of existing and advanced aircraft can be improved and thereby their operational capabilities can be enhanced. The idea behind all the wingtip devices is to diffuse the strong vortices released at the tip and optimise the span wise lift distribution, while maintaining the additional moments on the wing within certain limits. For this purpose one should be able to produce favorable effects of the flow field using wing tip and reducing the strength of the trailing vortex with the aid of wingtip devices, e.g., winglets, wing tips of complex plan-form, sails, and various modifications of the wingtip side edge.

Modern interest in winglets spans the last 25 years. In July 1976, Whitcomb[1-2] of NASA Langely Research Centre published a general design approach that summarised the aerodynamic technology involved in winglet design. Small and nearly vertical fins were installed on wings of KC-135A aircraft and flight was tested in 1979 and 1980. Whitcomb showed that winglets could increase an aircraft's range by as much as seven percent at cruise speeds. A NACA contract [3] in the 1980s assessed winglets and other drag reduction devices, and they found that wingtip devices (winglet, feathers, sails, etc.) could improve drag due to lift efficiency by 10 to 15% if they are designed as an integral part of the wing.

The "spiroid" wingtip [4] produces a reduction in induced drag at the same time blended winglet [5] reduces drag by eliminating the discontinuity between the wing tip and the winglet. A smoothed version is used on the gently upswept winglet of the Boeing 737-400. Boeing Business Jets and Aviation Partners, Inc. have embarked upon a cooperative program to market conventional winglets for retrofiting to the Boeing 7xx series of jetliners. Flight tests on the Boeing Business Jet 737-400 resulted in a 7% drag reduction. Theoretical predictions had indicated that the configuration would have only a 1-2% improvement, and wind tunnel tests had shown only 2% drag reduction [6]. This indicates that wind tunnel test results of winglet configurations should be reviewed with some caution.

The first industrial application of the winglet concept was in sailplane. The Pennsylvania State University (PSU) 94-097 airfoil has been designed for use on winglets of high-performance sailplanes [7]. To validate the design tools, as well as the design itself, the airfoil was tested in the Pennsylvania State Low-Speed, Low-Turbulence Wind Tunnel from Reynolds numbers of 2.4 x 10^5 to 1.0 x 10^6. Performance predictions from two well-known computer codes are compared to the data

NOMENCLATURE

c	Airfoil chord (m)
α	Angle-of-attack ($^\circ$)
D	Drag force (N)
L	Lift force (N)
M	Pitching moment (Nm)
ρ_∞	Air density (kg/m^3)
S	Reference area (m^2)
V_∞	Free stream velocity (m/s)
q_∞	Dynamic pressure (Pa)
C_D	Drag coefficient
C_L	Lift coefficient
C_M	Pitching moment coefficient
C1	Load No. 1
C2	Load No. 2
C3	Load No. 3
C4	Load No. 4
C5	Load No. 5
C6	Load No. 6

obtained experimentally, and both are found to generate results that are in good agreement with the wind tunnel measurements.

To improve the performance of a wing, the multi-winglet [8] design was evaluated to demonstrate its advanced performance potential over the baseline wing, an equivalent single winglet. The results of their wind tunnel testing show that certain multi-winglet configurations reduced the wing induced drag and improved L/D by 15-30% compared to the baseline 0012 wing. In Europe, an extension to the wing tip airfoils called Wing-Grid has been developed [9]. Wing-Grid is a set of multiple wing extensions added to the wing. These small wings are added at various angles so that their tip vortices do not interact to form a strong vortex. These smaller vortices dissipate the vortex energy so that the lift distribution is modified and the induced drag of the wing is reduced. But this concept is limited, since it is not able to change configuration in flight to optimise drag reduction.

The aerodynamic characteristics for the aircraft model with NACA wing No. 65-3-218 have been presented in this paper. The study on the enhanced performance of the aircraft models is also given by incorporating winglets of different configurations.

MATERIALS AND METHODS

a) Wind Tunnel, Model Details and Instrumentation

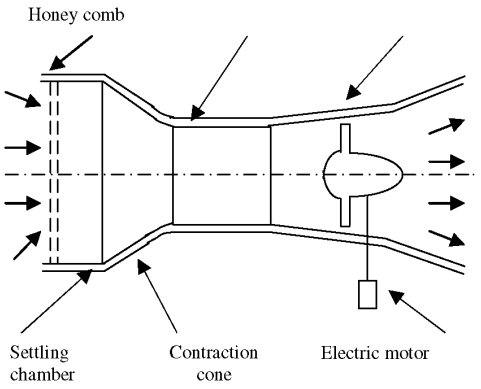

Figure 1: Schematic diagram of open loop low speed wind tunnel (OLWT-1000)

A Subsonic wind tunnel of 1000 mm x1000 mm rectangular test section and 2500 mm long at Aerodynamics Laboratory of the Faculty of Engineering (Universiti Putra Malaysia) is used for carrying out the experiments. The wind tunnel (Figure 1) can be operated at a maximum air speed of 50 m/s and the turntable has a capacity for setting an angle of attack of 14 degree. The aircraft model used for the present study consists of a cylindrical body with NACA 65-3-218 airfoil rectangular wing. The aircraft model has a span of 0.66 m and a chord of 0.121m. The elliptical shaped winglets (Figure 2) were designed to be made of wood with chord length of 0.121m, which matches the chord length of the wing. Figure 3 shows a photograph of the aircraft model with elliptical shaped winglet, which is mounted horizontally in the test section of the wind tunnel.

The tests are conducted with free-stream velocity of 21.36 m/s, 26.76 m/s, and 32.15 m/s with and without elliptical winglet. The ambient pressure, temperature and humidity were

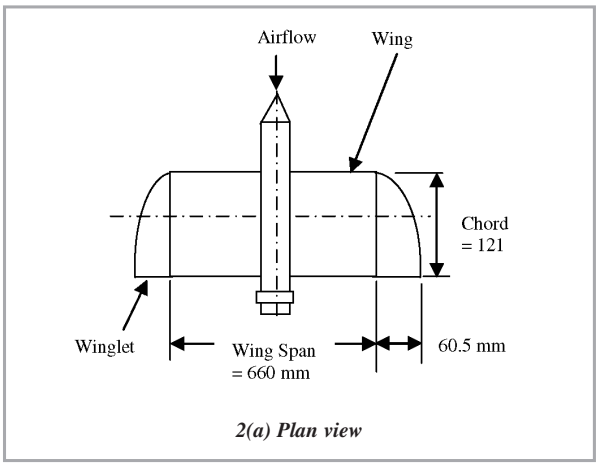

Figure 2: Schematic diagram of the aircraft model with the winglet at 600 inclination

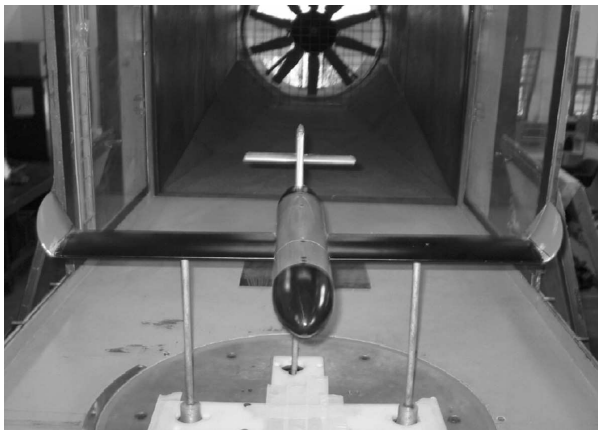

Figure 3: Aircraft model with elliptical winglet

recorded using barometer, thermometer, and hygrometer respectively for the evaluation of air density in the laboratory environment. Longitudinal tests were carried out at an angle of attack ranging from zero degree to 14 degree with an increment of 2 degree. During the test the pitching moment, lift and drag forces were measured using the six-component external balance and the coefficients of lift, drag and moment are obtained using the Equation (1-3) [10-11] given below,

Coefficient of lift is defined as

$$C_L = \frac{L}{\frac{1}{2}\rho_\infty V_\infty^{\ 2} S} \quad (1)$$

Coefficient of drag is defined as

$$C_D = \frac{D}{\frac{1}{2}\rho_\infty V_\infty^{\ 2} S} \quad (2)$$

Coefficient of pitching moment is defined as

$$C_M = \frac{M}{\frac{1}{2}\rho_\infty V_\infty^{\ 2} Sc} \quad (3)$$

b) Calibration Details

Calibration of the balance:

The objective of the calibration is to revalidate the calibration matrix and compare it with the calibration matrix data provided by the manufacturer of the six-component external balance. Figure 4 shows the drawing of a calibration rig/fixture used for the validation of calibration matrix.

The calibration rig/fixture is to be mounted on the upper platform of the balance in place of a model. To check the calibration of the six-component external balance, the following procedure is adopted.

The amount of loads to be applied step by step at the various locations shown on the calibration rig is given in Table 1. For the loads applied against the individual step e.g. step I (Table1), the equivalent forces and moments are calculated in the X, Y, and Z directions and they are given in Table 2. The corresponding sensor readings from all the load cells are noted and given against the step I, in the first row of Table 3. The same procedure is followed for obtaining the sensor readings for the other steps e.g. steps II to VI and they are also given in Table 3.

The relationship between signal readings and the loads applied on the calibration rig are given by the following matrix equation.

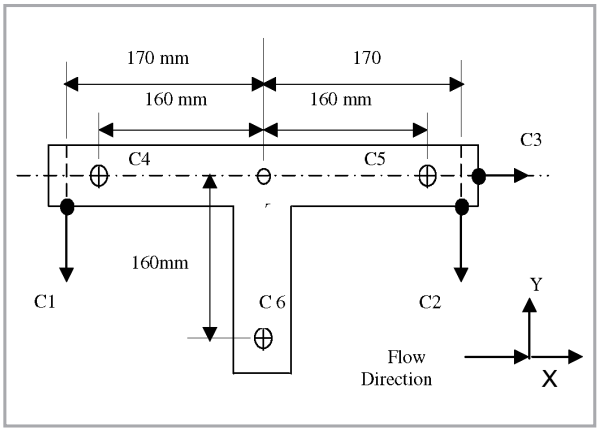

Figure 4: Plan view of the calibration rig

Table 1: Calibration loads applied at different load locations

Step No.	Loads at load locations					
	C1 (kg_f)	C2 (kg_f)	C3 (kg_f)	C4 (kg_f)	C5 (kg_f)	C6 (kg_f)
Step I	0.984	0	0	0	0	0
Step II	0.984	1.975	0	0	0	0
Step III	0	0	1.975	0	0	0
Step IV	0	0	0	1.975	0	0
Step V	0	0	0	0.984	1.975	0
Step VI	0	0	0	0	0	1.975

Table 2: Equivalent forces and moments for different load locations

Step No.	Equivalent Force			Equivalent Moment		
	F_X (kg_f)	F_Y (kg_f)	F_Z (kg_f)	M_X (kg_f m)	M_Y (kg_f m)	M_Z (kg_f m)
Step I	0	-0.984	0	-0.100	0	0.167
Step II	0	-2.959	0	-0.300	0	-0.168
Step III	1.975	0	0	0	-0.200	0
Step IV	0	0	-1.975	0	-0.316	0
Step V	0	0	-2.959	0	0.159	0
Step VI	0	0	-1.975	0.316	0	0

$$\{L_i\} = [K_{ij}]\ \{F_i\} \quad (4)$$

Where, $[K_{ij}]$ is the coefficient matrix.
$\{L_i\}$ is the signal matrix.
$\{F_i\}$ is the load matrix.

Table 3: Sensor readings corresponding to load applied at different locations of the calibration rig

Step no.	Sensor Readings					
	L1 Volts	L2 Volts	L3 Volts	L4 Volts	L5 Volts	L6 Volts
Step I	-0.032	-1.330	2.311	-1.492	1.461	-0.008
Step II	0.115	4.051	-0.720	-4.972	4.981	-0.044
Step III	-2.724	-0.177	0.175	-2.450	-2.474	4.819
Step IV	-0.003	0.029	-0.072	1.128	1.065	-0.238
Step V	-0.012	-0.017	-0.028	0.683	0.627	1.618
Step VI	-0.010	-0.018	-0.006	-0.257	1.460	0.749

Using the data of loads applied, F_i at the calibration rig (Table 2) and the corresponding signal output, L_i (Table 3), six equations obtained for step I. In this way the 36 equations are

obtained using the applied load and observed signal data of all the steps in terms of 36 unknowns. These unknowns are solved using MAT Lab software giving the coefficient matrix K_{ij}. The calibration matrix is obtained by finding the inverse of the coefficient matrix K_{ij}.

RESULTS AND DISCUSSIONS

Wind-tunnel measurements were done using the aircraft model at Reynolds numbers $1.7x10^5$, $2.1x10^5$, and $2.5x10^5$. The lift coefficient characteristics of the aircraft model under test are shown in Figure 5 for all Reynolds numbers. The lift increases with increase in angle of attack to a maximum value and thereby decreases with further increase in angle of attack. The initial value of lift coefficient at zero angle of attack for $1.7x10^5$ Reynolds number is 0.237 and the corresponding values of the lift coefficient for the Reynolds numbers $2.1x10^5$, and $2.5x10^5$ are 0.259 and 0.306 respectively. The maximum values of the lift coefficient for the above three Reynolds numbers are 0.805, 0.817, and 0.879 respectively and all these maximum values occur at an angle of attack of 8 degree. The maximum value of the lift coefficient appears to increase with the increase in Reynolds number. The experiments have been done up to an angle of attack of 14 degree. At the maximum value of the angle of attack the lift coefficient characteristic has a mixed behavior e.g. the value of the lift coefficient first decreases with increase in Reynolds number and then increases with further increase in Reynolds number. At the maximum angle of attack of 14 degree the lift coefficients are 0.657, 0.584, and 0.733 respectively for the Reynolds numbers of $1.7x10^5$, $2.1x10^5$, and $2.5x10^5$.

The reason for a drop in lift coefficient beyond a certain angle of attack e.g. 8^o is probably due to the flow separation, which occurs over the wing surface instead of having a streamlined laminar flow there. This condition is called stalling condition and the corresponding angle of attack is called stalling angle. The stalling angle happens to be approximately 8^0 for all the Reynolds numbers under the present study. The slope of the linear portion $a_0 = \frac{dc_L}{d\alpha}$ is called the lift slope and its values are 3.72, 4.01, and 4.11 respectively for the three Reynolds numbers under study.

The lift coefficient data for elliptical winglet for the two configurations i.e. configuration 1 (winglet inclination 0^o), and configuration 2 (winglet inclination 60^o) are given in Figures 6 and 7 respectively. In the case of the winglet for both configurations 1 and 2 a similar pattern is observed. In general it is observed that the coefficient of lift increases with the increase of Reynolds number. For the maximum Reynolds number of $2.5x10^5$ the lift coefficients for configuration-1 (Figure 6) and for configuration-2 (Figure 7) are 0.934 and 1.018 respectively corresponding to an angle of attack of 8^0 which is also the stall angle of attack. The other details of the lift coefficients are given in Table 4.

The drag coefficients of the aircraft model under test for all Reynolds numbers are shown in Figure 8. The drag increases slowly with increase in angle of attack to a certain value and then it increases rapidly with further increase in angle of attack. The initial value of drag coefficient at zero angle of attack for $1.7x10^5$ Reynolds number is 0.085 and the corresponding values of the drag coefficient for the Reynolds numbers $2.1x10^5$, and $2.5x10^5$ are 0.083 and 0.065 respectively. The values of the drag coefficient at the transition point i.e. at an angle of attack of 4 degree for the above three Reynolds numbers are 0.104, 0.100, and 0.085 respectively. The value of the drag coefficient appears to decrease with the increase in Reynolds number. The experiments have been done up to an angle of attack of 14

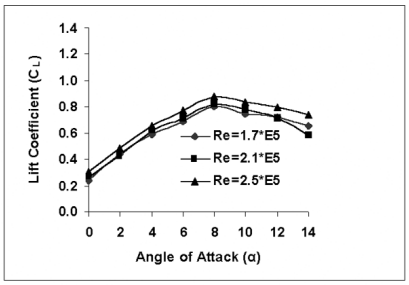

Figure 5: Lift coefficients for the aircraft model without winglet

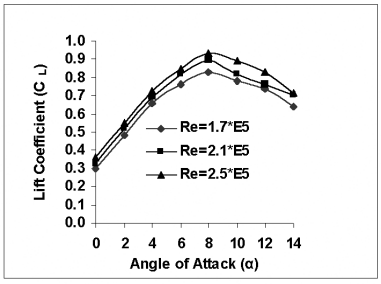

Figure 6: Lift coefficients for the aircraft model with elliptical winglet at 0^o (Configuration 1)

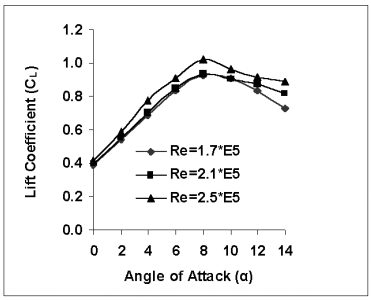

Figure 7: Lift coefficients for the aircraft model with elliptical winglet at 60^o (Configuration 2)

Table 4: Lift coefficients from experimental data

Serial Number	Winglet Configuration	Reynolds Number 10^5	Lift coefficient, C_L		
			Initial Angle of Attack 0^0	Stall Angle of Attack 8^0	Final Angle of Attack 14^0
1	Without Winglet	1.7	0.237	0.805	0.657
		2.1	0.259	0.817	0.584
		2.5	0.306	0.879	0.733
2	Elliptical Winglet, Configuration 1 (0^0 angle)	1.7	0.299	0.829	0.641
		2.1	0.327	0.889	0.700
		2.5	0.359	0.934	0.713
3	Elliptical Winglet, Configuration 2 (60^0 angle)	1.7	0.386	0.930	0.729
		2.1	0.394	0.934	0.815
		2.5	0.416	1.018	0.885

degree. At the maximum value of the angle of attack the drag coefficient characteristic has a mixed behaviour e.g. the value of the drag coefficient decreases with increase in Reynolds number and then increases with further increase in Reynolds number. At the maximum angle of attack of 14 degree the drag coefficients are 0.249, 0.275, and 0.211 respectively for the Reynolds numbers of $1.7x10^5$, $2.1x10^5$, and $2.5x10^5$. The rapid increase in drag coefficient, which occurs at higher values of angle of attack, is probably due to the increasing region of separated flow over the wing surface, which creates a large pressure drag.

Table 5: Drag coefficients from experimental data

Serial Number	Winglet Configuration	Reynolds Number 10^5	Drag coefficient, C_D		
			Initial Angle of Attack 0^0	Transition Angle of Attack 4^0	Final Angle of Attack 14^0
1	Without Winglet	1.7	0.085	0.104	0.249
		2.1	0.083	0.100	0.275
		2.5	0.065	0.085	0.211
2	Elliptical Winglet, Configuration 1 (0^0 angle)	1.7	0.053	0.058	0.136
		2.1	0.050	0.056	0.140
		2.5	0.049	0.053	0.128
3	Elliptical Winglet, Configuration 2 (60^0 angle)	1.7	0.070	0.078	0.166
		2.1	0.058	0.065	0.153
		2.5	0.047	0.060	0.134

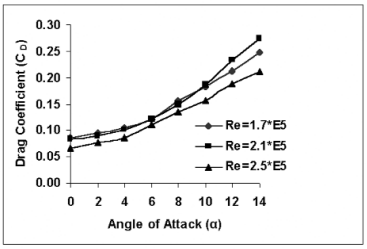

Figure 8: Drag coefficients for the aircraft model without winglet

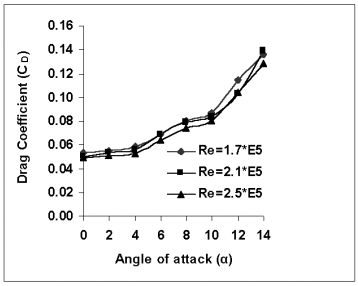

Figure 9: Drag coefficients for the aircraft model with elliptical winglet 0^o (Configuration 1)

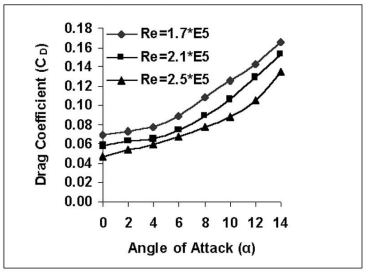

Figure 10: Drag coefficients for the aircraft model with elliptical winglet 60^o (Configuration 2)

The drag coefficient data for elliptical winglet for the two configurations i.e. configuration 1 (winglet inclination 0^o), and configuration 2 (winglet inclination 60^o) are given in Figures 9 and 10. In the case of elliptical winglet for both configurations 1 and 2 a similar pattern has been observed. In general it is observed that the coefficient of drag decreases with the increase of Reynolds number. For maximum Reynolds number of $2.5x10^5$ and at 0^0 angle of attack the drag coefficients for the elliptical winglet of configuration-1 (Figure 9) and elliptical winglet of configuration-2 (Figure 10) are 0.049 and 0.047 respectively. The other details of the drag coefficients are given in Table 5.

The pitching moment coefficients of the aircraft model under test for all Reynolds numbers are shown in Figure 11. The moment coefficient curve is nearly linear over most of the practical range of the angle of attack (0^o to 6^o); that is, the slope of the moment coefficient curve, $m_0 = \frac{dc_M}{d\alpha}$ is essentially constant. The initial value of pitching moment coefficient at zero angle of attack for $1.7x10^5$ Reynolds number is -0.075 and the corresponding values of the pitching moment coefficient for the Reynolds numbers $2.1x10^5$, and $2.5x10^5$ are -0.089 and -0.110 respectively. The values of the pitching moment coefficient at the transition point i.e. at an angle of attack of 6 degrees for the above three Reynolds numbers are -0.098, -0.135, and -0.161 respectively. The variation becomes nonlinear at high angle of attack, when the flow separates from the top surface. As shown in the case of the moment curves, the linear portion of the moment curves have very small effects of Reynolds numbers. The pitching moment decreases rapidly with increase in angle of attack to a certain value and then it decreases more rapidly with further increase in angle of attack. The value of the pitching moment coefficient appears to decrease with the increase in Reynolds number. The experiments have been done up to an angle of attack of 14 degree. At the maximum angle of attack of 14 degree the pitching moment coefficients are -0.370, -0.493, and -0.632 respectively for the Reynolds numbers of $1.7x10^5$, $2.1x10^5$, and $2.5x10^5$. The rapid decrease in pitching moment coefficient, which occurs at higher values of angle of attack, is probably due to the increasing region of separated flow over the wing surface.

The pitching moment coefficient data for elliptical winglet for the two configurations i.e. configuration 1 (winglet inclination 0^o), and configuration 2 (winglet inclination 60^o) is given in Figures 12 and 13. In the case of elliptical winglet for both configurations 1 and 2 a similar pattern has been observed. In general it is observed that the coefficient of pitching moment decreases with the increase of Reynolds number. For maximum Reynolds number of $2.5x10^5$ and at 0^o angle of attack the pitching moment coefficients for the elliptical winglet of configuration-1 (Figure 12) and elliptical winglet of configuration-2 (Figure 13) are -0.100 and -0.359 respectively. At the range of the angle of attack 8^0 to 14^0 the pitching moment coefficient characteristic has a mixed behaviour e.g. the value of the pitching moment coefficient decreases with increase in Reynolds number and then increases with further increase in Reynolds number. The other details of the pitching moment coefficients are given in Table 6.

The values of the lift/drag ratio of the aircraft model under test are shown in Figure 14 for all the Reynolds numbers considered in this study. The lift/drag ratio increases with increase in angle of attack to its maximum value and thereby it decreases with further

Table 6: Pitching moment coefficients from experimental data

Serial Number	Winglet Configuration	Reynolds Number 10^5	Pitching moment coefficient, C_M		
			Initial Angle of Attack 0^0	Transition Angle of Attack 6^0	Final Angle of Attack 14^0
1	Without Winglet	1.7	-0.075	-0.098	-0.370
		2.1	-0.089	-0.135	-0.493
		2.5	-0.110	-0.161	-0.632
2	Elliptical Winglet, Configuration 1 (0^0 angle)	1.7	-0.068	-0.106	-0.400
		2.1	-0.082	-0.132	-0.440
		2.5	-0.100	-0.158	-0.636
3	Elliptical Winglet, Configuration 2 (60^0 angle)	1.7	-0.292	-0.367	-0.971
		2.1	-0.330	-0.413	-0.998
		2.5	-0.356	-0.414	-0.976

Table 7: Lift/Drag ratio experimental data

Serial Number	Winglet Configuration	Reynolds Number 10^5	Lift/Drag ratio (L/D)			
			Initial Angle of Attack 0^0	Transition Angle of Attack 4^0	Transition Angle of Attack 6^0	Final Angle of Attack 14^0
1	Without Winglet	1.7	2.8	5.7	5.7	2.6
		2.1	3.1	6.1	5.9	2.1
		2.5	4.7	7.71	7.0	3.5
2	Elliptical Winglet Configuration 1 (0^0 angle)	1.7	5.61	11.27	11.09	4.73
		2.1	6.53	12.30	11.84	5.02
		2.5	7.33	13.73	13.19	5.55
3	Elliptical Winglet Configuration 2 (60^0 angle)	1.7	5.5	8.8	9.3	4.4
		2.1	6.7	10.8	11.4	5.3
		2.5	8.8	13.0	13.5	6.6

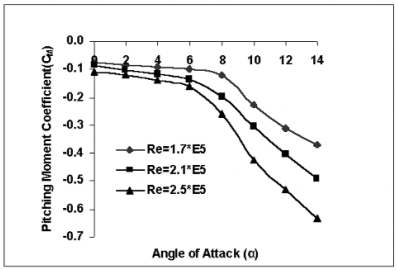

Figure 11: Pitching moment coefficients for the aircraft model without winglet

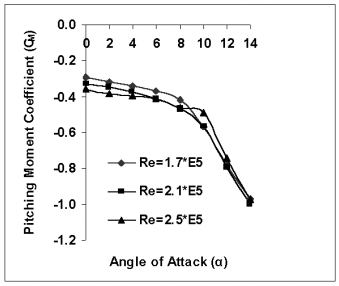

Figure 13: Pitching moment coefficients for the aircraft model with elliptical winglet 60° (Configuration 2)

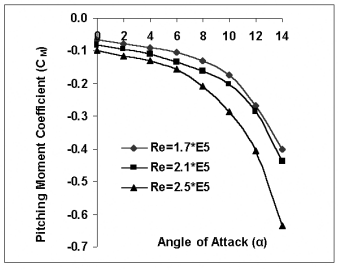

Figure 12: Pitching moment coefficients for the aircraft model with elliptical winglet (Configuration 1)

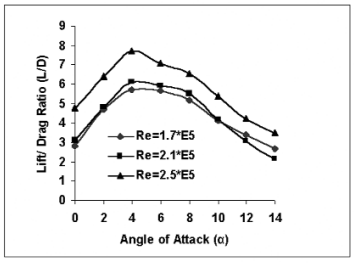

Figure 14: Lift/Drag ratio for the aircraft model without winglet.

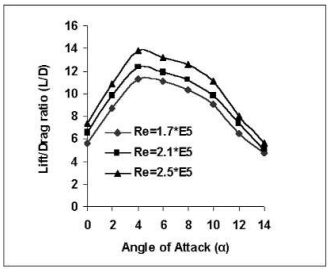

Figure 15: Lift/Drag ratio for the aircraft model with elliptical winglet 0° (Configuration 1)

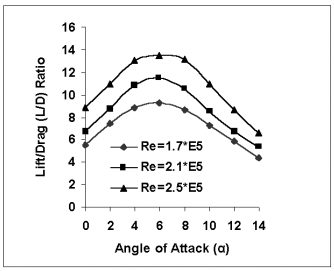

Figure 16: Lift/Drag ratio for the aircraft model with elliptical winglet 60° (Configuration 2)

increase in the angle of attack for the aircraft model. The initial value of the lift/drag ratio at zero angle of attack for $1.7x10^5$ Reynolds number is 2.8 and the corresponding values of the lift/drag ratio for the Reynolds numbers $2.1x10^5$, and $2.5x10^5$ are 3.1 and 4.7 respectively. The maximum values of the lift/drag ratio are 5.7, 6.1, and 7.71 for the above three Reynolds numbers respectively and all these maximum values occur at an angle of attack of 4 degrees. At the maximum value of the angle of attack the lift/drag ratio has a mixed behaviour e.g. the value of the lift/drag ratio first increases with increase in Reynolds number and then decreases with further increase in Reynolds number. At the maximum angle of attack of 14 degree the lift/drag ratios are 2.6, 2.1, and 3.5 respectively for the Reynolds numbers of $1.7x10^5$, $2.1x10^5$, and $2.5x10^5$.

The lift/drag ratio data for elliptical winglet for the two configurations i.e. configuration 1 (winglet inclination 0^0), and configuration 2 (winglet inclination 60^0) and given in Figures 15 and 16. In the case of elliptical winglet for both configurations 1 and 2 a similar pattern is observed. For a Reynolds number of $2.5x10^5$ the maximum values of the lift/drag ratio for elliptical winglet of configuration-1 (Figure 15) have been observed at an angle of attack of 4^0 and the respective value is 13.73 whereas for elliptical winglet of configuration-2 (Figure 16) the maximum value occurs at an angle of attack of 6^0 and the respective value is 13.5. The other details of the lift/drag ratio at other angle of attacks are given in Table 7 considered in this study.

CONCLUSIONS

Following are the conclusions drawn from this investigation,

i) Aerodynamic characteristics for the aircraft model with NACA wing No. 65-3-218 have been presented.

ii) Lift curve slope increases more with the addition of the elliptical winglet and at the same time the drag decreases more for the aircraft model with elliptical shaped winglet giving an edge over the aircraft model without winglet as far as L/D for the elliptical winglet is considered.

iii) Elliptical winglet of configuration 2 (Winglet inclination 60^0) has, overall, the best performance, giving about 6% increase in lift curve slope as compared to without winglet and it is giving the best lift/drag ratio.

AKNOWLEDGEMENTS

The authors are grateful for the support provided by grants from the IRPA (Project No: 09-02-04-0446-EA001), and the Aerodynamics Laboratory of the University Putra Malaysia for using the Wind Tunnel. ■

REFERENCES

[1] Whitcomb R.T., *"A Design Approach and Selected Wind-Tunnel Results at High Subsonic Speeds for Wing-Tip Mounted Winglets"*, NASA TN D-8260, July 1976.

[2] Whitcomb R. T., *"Methods for Reducing Aerodynamic Drag,"* NASA Conference Publication 2211, Proceedings of Dryden Symposium, Edwards, California, 16 September 1981.

[3] Yates, John E., and Donaldson, Coleman dup., *"Fundamental Study of Drag and an Assessment Of Conventional Drag-Due-To-Lift Reduction Devices,"* NASA Contract Rep 4004, September 1986.

[4] Louis B. Gratzer, *"Spiroid-Tipped Wing,"* U. S. patent 5, 102,068, 7 April 1992.

[5] Reginald V. French, *"Vortex Reducing Wing Tip,"* U. S. Patent 4, 108,403, 22 August 1978.

[6] Clark Joe, *"Aviation Partners, Inc.,"* 12 July 1999.

[7] Maughmer M. D., Tmothy S. Swan and Willits M., *"The Design and Testing of a Winglet Airfoil for Low-Speed Aircraft,"* AIAA Paper 2001-2478, June 2001.

[8] Smith M. J., Komerath N., Ames R., Wong O., and Pearson J., *"Performance Analysis of a Wing with Multiple Winglets,"* AIAA Paper-2001-2407, 2001.

[9] Roche La. U., and Palffy S., *"WING-GRID, a Novel Device for Reduction of Induced Drag on Wings,"* Proceedings of ICAS 96, Sorrento, September 8-13, 1996.

[10] Bertin John J., *Aerodynamics for Engineers*, New Jersey, Prentice-Hall, Inc., 2002.

[11] Hossain, A. *"Investigations of Longitudinal Aerodynamic Characteristics of Aircraft Model with and without Winglet"*, M.Sc. Thesis, (Submitted) Department of Aerospace Engineering, Universiti Putra Malaysia, UPM Serdang, Selangor, Malaysia, 2004.

PROFILES

Assoc. Prof. Dr Prithvi Raj Arora
Aerospace Engineering Department,
Faculty of Engineering,
Universiti Putra Malaysia ,
43400 UPM, Serdang,
Selangor.

Phone: 603-8946 6404(O)
Fax: 603-8656 7125
Email: Prithvi@eng.upm.edu.my;
Prithviraj.arora@gmail.com

The author has obtained a B.Sc. Engineering degree (Mechanical) in 1966 from Jiwaji University, Gwalior (India). Subsequently earned M.Sc. (Faculty of Engineering) by thesis in 1970 and PhD (Faculty of Engineering) in 1985 by thesis both from Indian Institute of Science, Bangalore (India). The author has worked at Mechanical Engineering Department of Indian Institute of Science, Bangalore (India) from 1970 as Research Assistant to 1996 as Principal Research Scientist. His research areas of interest are Design of special purpose machines, Characterisation of materials, Fatigue and fracture mechanics, Failure analysis, and Stress analysis. The author has been working at Aerospace Engineering Department, Faculty of Engineering, Universiti Putra Malaysia Since December 1996 as Associate Professor. Currently the author has been actively involved in the research related with Fretting Fatigue, Fracture Mechanics, and Characterisation of materials.

Ir. Prasetyo Edi, MSc., PhD.
Department of Aerospace Engineering,
Faculty of Engineering,
Universiti Putra Malaysia ,
43400 UPM, Serdang,
Selangor.

Phone: 603-8946-6396(O)
Fax: 603-8656 7125
Email: p_edi@eng.upm.edu.my;
edi_phd@yahoo.com

The author has obtained an IR. (B.Sc.) Engineering degree (Mechanical) in 1986 from Gadjah Mada University, Jogjakarta, Indonesia. From July 1986 until March 2003, He has been working for Indonesian Aerospace (IAe). The author last job with IAe is Manager for Product and Method Innovation. The author earned M.Sc. (Aerospace Vehicle Design) by thesis in 1994 and PhD (Air Vehicle Technology) in 1998 by thesis both from Cranfield University, Cranfield, Bed's, UK. His research areas of interest are aircraft configuration design, wing design, aerodynamic, Multidisciplinary Design/Optimization, and Unmanned Aerial Vehicle (UAV). The author has been working at Aerospace Engineering Department, Faculty of Engineering, Universiti Putra Malaysia since April 2003 as Lecturer. Currently the author has been actively involved in the research related with Unmanned Aerial Vehicle (UAV), aircraft configuration design, wing design and aerodynamic.

A. Hossain
Department of Aerospace Engineering,
Universiti Putra Malaysia,
43400 UPM Serdang,
Selangor.

Thamir S. Younis
Department of Mechanical Engineering,
Universiti Putra Malaysia,
43400 UPM Serdang,
Selangor.

M. Saleem
Department of Aerospace Engineering,
Universiti Putra Malaysia,
43400 UPM Serdang,
Selangor.